

# Fluorescence of Horse Liver Alcohol Dehydrogenase Using One- and Two-Photon Excitation

Joseph R. Lakowicz,<sup>1,3</sup> Borys Kierdaszuk,<sup>1,2</sup> Ignacy Gryczynski,<sup>1</sup> and Henryk Malak<sup>1</sup>

Received December 2, 1994; accepted December 18, 1995

We examined the steady-state and time-resolved emission of liver alcohol dehydrogenase resulting from one-photon and two-photon excitation. Previous studies with one-photon excitation revealed that the two nonidentical tryptophan residues display different emission spectra and decay times. The use of two-photon excitation resulted in similar emission spectra, multiexponential intensity decays, time-resolved emission spectra, and anisotropy decays as was observed for one-photon excitation. These results suggest that both nonidentical tryptophan residues are excited to a similar extent for one- and two-photon excitation. However, the limiting anisotropy ( $r_0$ ) with two-photon excitation from 585 to 610 nm is below 0.1 and appears distinct from that observed previously for *N*-acetyl-L-tryptophanamide.

**KEY WORDS:** Fluorescence; anisotropy; one-photon excitation; two-photon excitation; anisotropy spectra; horse liver alcohol dehydrogenase; time-resolved fluorescence; proteins; tryptophan.

## INTRODUCTION

The intrinsic tryptophan emission of proteins is known to depend on the local environment of the trp residues and to be sensitive to minor changes in protein conformation. In recent years there has been considerable effort to correlate the spectral properties with structural features of proteins with the time-resolved fluorescence data. One of the best-known examples is horse liver alcohol dehydrogenase, which has been extensively studied by several groups, as summarized by Eftink.<sup>(1)</sup>

Liver alcohol dehydrogenase (LADH)<sup>4</sup> is a homodimeric protein, with each monomer having 374 amino acids and a mass of 40 kD. It is known that this protein contains two tryptophan residues per subunit, trp-15 and trp-314, and their location is well-known from the crystal structure of LADH and several of its derivatives and binary complexes.<sup>(2-6)</sup> Trp-15 is located at the outer edge of the catalytic domain and its side chain is accessible to solvent as well as to dynamic quenching by iodide<sup>(7,8)</sup> and acrylamide.<sup>(9)</sup> Trp-314 is located in the apolar intersubunit region of catalytic domain formed by  $\beta$ -sheet structures from each subunit, and these residues are inaccessible to water-soluble quenchers. Apolar side chains of Val-290, Leu-303, and Met-301 from its own subunit and Met-303 and Leu-308 from the second subunit have been shown to be in close contact with trp-314, mostly excluding trp-314 from interaction with solvent. The indole rings of trp-314 residues from two subunits are close to one another and the center-to-center distance between them ( $\sim 7$  Å) suggests the possibility of energy transfer, but the experimental data argue against significant homotransfer.<sup>(1)</sup> The tryptophan fluo-

<sup>1</sup> Center for Fluorescence Spectroscopy, Department of Biological Chemistry, University of Maryland School of Medicine, 108 North Greene Street; Baltimore, Maryland 21201.

<sup>2</sup> Department of Biophysics, University of Warsaw, 93 Zwirki i Wigury Street, PL-02089 Warsaw, Poland.

<sup>3</sup> To whom correspondence should be addressed.

<sup>4</sup> Abbreviations used: LADH, liver alcohol dehydrogenase;  $\beta$ -NAD<sup>+</sup>,  $\beta$ -nicotinamide adenine dinucleotide; OPE, one-photon excitation; OPIF, one-photon induced fluorescence; TPE, two-photon excitation; TCSPC, time-correlated single photon counting; TPIF, two-photon induced fluorescence.

rescence of LADH has also been characterized by time-resolved methods. Data from many laboratories<sup>(10-14)</sup> showed a biexponential decay of LADH fluorescence with a short-lived component (3.4–3.8 ns) from trp-314 and a long-lived component (6.7–7.45 ns) from trp-15.

In recent years, there has been an increased interest in the use of two-photon excitation to provide additional information on proteins and other biological macromolecules.<sup>(15-23)</sup> Because of the extensive data on LADH for one-photon excitation, we chose this protein for use with two-photon excitation. In particular, we questioned whether the two tryptophan residues would be excited to similar or different extents with one-photon excitation (OPE) and two-photon excitation (TPE). Additionally, it was not known whether the low anisotropy value observed for indoles with two-photon excitation would also be observed for an indole residue in a nonpolar environment (i.e., trp-314). While indole and *N*-acetyl-L-tryptophanamide have been studied by TPE in viscous polar solvents,<sup>(23)</sup> no information is available on the effects of local environment on the cross section for TPE. We expected the different intensity decay times of the two tryptophan residues in LADH to provide an indication of the extent of excitation of each residue by OPE and TPE. For these reasons LADH provided an ideal protein to determine whether one can expect selective excitation or other additional information from the two-photon indirect fluorescence of proteins.

## MATERIALS

Horse liver alcohol dehydrogenase (LADH; EC 1.1.1.1), lot number 12388822-60, was obtained from Boehringer Mannheim (Germany) as a crystalline suspension in 20 mM phosphate buffer (pH 7) containing 10% ethanol. The crystalline suspension was dissolved in an excess of 20 mM phosphate buffer (pH 7.5) and further purified with a 70% yield with repeated use of Centriprep-10 Concentrators (Amicon, Inc., Beverly, MA) to exchange buffer and to remove low molecular weight contaminations (MW <10 kD). These lower molecular weight species showed absorption and emission in the range 250–290 and 300–380 nm, respectively. Undissolved material was also removed by centrifugation. After desalting, the solution of LADH (~4 mg/ml) in 20 mM phosphate buffer (pH 7.5) was heated at 50°C for 15 min, and the resulting white flocculent precipitate (~25% of protein) was removed by centrifugation. The heat-treated LADH solution remained clear for at least 3 weeks at 4°C without loss of activity (3.5 U/mg), which was equivalent in that expected for the 100% pure

enzyme. The concentration of LADH was measured spectrophotometrically as described using an optical density of 4.55 for absorption of 1% enzyme solution at 280 nm.<sup>(24)</sup> Activity of LADH was determined by the method of Vallee and Hoch<sup>(25)</sup> using the rate of increase in absorbency at 340 nm, caused by the reduction of 8 mM  $\beta$ -NAD<sup>+</sup> in 10 mM sodium pyrophosphate buffer (pH 8.8) containing 0.6 M ethanol as the substrate. One unit is defined as the amount of enzyme that reduces 1  $\mu$ mol of  $\beta$ -NAD<sup>+</sup>/min at 25°C, pH 8.8.

Glycerol (p.a.) was bought from Janssen Chimica through Spectrum Chemical Mfg Corp. (New Brunswick, NJ). Disodium and tetrasodium pyrophosphates and  $\beta$ -nicotinamide adenine dinucleotide were obtained from Sigma Chemical Co. Mono- and disodium phosphates were purchased from Fisher Scientific Co. (New Jersey, NJ). Phosphate buffer (pH 7.5) was made using Milli-Q water. All other chemicals, reagents, and materials were of the highest, spectral-grade quality commercially available. They were checked by UV absorption and/or fluorescence measurements. Absorption measurements were performed on a Perkin-Elmer Lambda 6 UV/VIS spectrophotometer (Perkin-Elmer Co., Rockville, MD). Steady-state fluorescence measurements were carried out at 20°C using a SLM 8000 photon-counting spectrofluorimeter (with 2-nm spectral resolution for excitation and emission) equipped with a Hamamatsu R928 photomultiplier tube. Fluorescence was excited at several wavelengths in the range 270–300 nm, and fluorescence spectra were recorded in the range 280–400 nm.

## FLUORESCENCE SPECTROSCOPIC METHODS

Two-photon excitation was accomplished using the fundamental output of a cavity-dumped rhodamine-6G laser from 566 to 610 nm, which was passed through a Glan-Thompson vertical polarizer and focused in the sample using a 5-cm-focal length lens. The pulse full width at half-maximum was about 5 ps at a repetition rate of 3.795 MHz. One-photon-induced fluorescence and excitation anisotropy spectra were measured using the same laser system as two-photon-induced fluorescence and fluorescence anisotropy (see above) equipped additionally with a 390 Frequency Doubler (Spectra Physics) and a polarization rotator. For comparison of the steady-state emission spectra with OPE and TPE, we used an instrument for time-correlated single-photon counting.<sup>(26-27)</sup> The steady-state intensity at each wavelength was obtained by integrating the time-resolved intensity measurements. In addition to increased sensi-

tivity, the use of TCSPC allowed us to demonstrate the absence of scattered light in the detected emission. Use of the same instrumentation for both modes of excitation allowed direct comparison of the spectral data. We also made separate measurements of OPE and TPE emission spectra of LADH using the same laser system for samples placed in the SLM 8000 photon-counting spectrofluorometer, but with laser excitation. The same results were obtained using these two instruments.

The samples were contained in  $1.0 \times 0.5$ -cm cuvettes placed in the thermostated SLM cell holder (Urbana, Champaign, IL), with the long axis aligned along the incident light path and with the focal point positioned about 0.5 cm from the surface facing the incident light. The position of the cuvette and the lens were adjusted so that the focal point of the laser excitation was located near the observation window. Fluorescence was collected by a suprasil lens, filtered from the contaminating scatter of the long-wavelength light using two Corning 7-54 filters (3 mm thick each), and passed through an ISA (New Jersey) grating monochromator (4-nm slit bandwidth) and Glan-Thompson polarizer in the magic-angle position. The wavelength scale of the monochromator was calibrated using a SCT1 mercury lamp (Ultra-Violet Products Inc., San Gabriel, CA) as a wavelength standard. Fluorescence spectra were corrected for transmittance of the two 7-54 filters used to isolate the emission. The effect of the intensity of incident light on the one-photon- and two-photon-induced fluorescence intensity (Fig. 1, insert) was measured using a set of the neutral density filters to decrease the peak excitation intensity. Signal from the solvent alone was less than 0.5% and was subtracted from sample fluorescence.

For anisotropy determinations, the polarized emission was observed through an interference filter centered at 313 or 340 nm (10-nm band-pass), a Glan-Thompson polarizer, and two 7-54 filters. The anisotropy  $r$  values were determined from the polarized fluorescence intensities as

$$r = (gF_{vv} - F_{vh}) / (gF_{vv} + 2F_{vh}) \quad (1)$$

where  $F_{vv}$  is vertically polarized emission intensity with vertically polarized excitation, and  $F_{vh}$  is horizontally polarized emission with vertically polarized excitation. The instrumental correction factor,  $g$ , is equal to  $g = F_{hh}/F_{hv}$ , where  $F_{hh}$  is horizontally polarized emission intensity with horizontally polarized excitation, and  $F_{hv}$  is vertically polarized emission with horizontally polarized excitation. This  $g$  factor corrects for the small polarization bias of the optical system and photomultiplier. The  $g$  factor was usually within a few percent of 1.0. Ani-

sotropy values presented here were obtained as an average of at least three determinations.

Time-domain intensity decays were measured using magic-angle conditions using the same experimental apparatus used for the steady-state measurements. For each emission wavelength  $\lambda$ , intensity decays  $I(\lambda, t)$  were fit to the multiexponential model using

$$I(\lambda, t) = \sum_i \alpha_i(\lambda) e^{-t/\tau_i} \quad (2)$$

where  $\alpha_i$  are the amplitudes associated with the decay time  $\tau_i$ . The fractional intensity of each component in the decay is given by  $f_i(\lambda) = \alpha_i(\lambda)\tau_i / \sum_j \alpha_j(\lambda)\tau_j$ . The mean decay time  $\langle \tau \rangle$  is given by  $\langle \tau \rangle = \sum_j f_j(\lambda)\tau_j$ .

The impulse response functions [Eq. (2)] at each wavelength were used to calculate time-resolved emission spectra.<sup>(28,29)</sup> This requires normalization of the preexponential factors, so the time-integrated intensity represents the steady-state intensity  $F(\lambda)$  at each wavelength. Normalization is accomplished using the factor  $H(\lambda)$ , which is calculated using

$$H(\lambda) = \frac{F(\lambda)}{\int_0^{\infty} I(\lambda, t) dt} \quad (3)$$

$$= \frac{F(\lambda)}{\alpha_1(\lambda)\tau_1 + \alpha_2(\lambda)\tau_2 + \alpha_3(\lambda)\tau_3} \quad (4)$$

The normalized functions are given by

$$I'(\lambda, t) = \frac{H(\lambda) I(\lambda, t)}{\sum_i \alpha'_i(\lambda) e^{-t/\tau_i}} \quad (5)$$

where

$$\alpha'_i(\lambda) = H(\lambda) \alpha_i(\lambda) \quad (6)$$

For any desired time ( $t_i$ ), the time-resolved emission spectrum is obtained by plotting the values  $I'(\lambda, t_i)$  for each wavelength.

Frequency-domain intensity and anisotropy decays were obtained on the gigahertz instrument described previously.<sup>(30,31)</sup> Data were analyzed as described previously.<sup>(32-34)</sup> The differential phase and modulated anisotropy data were fit to a multiexponential anisotropy decay [ $r(t)$ ] model using

$$r(t) = \sum_j r_{0j} e^{-t/\theta_j} \quad (7)$$

where  $r_{0j}$  is the amplitude of the total anisotropy, which decays with a correlation time  $\theta_j$ , and the total anisotropy is given by ( $r_0 = \sum_j r_{0j}$ ). For analysis of the intensity decays the uncertainties in phase and modulation were

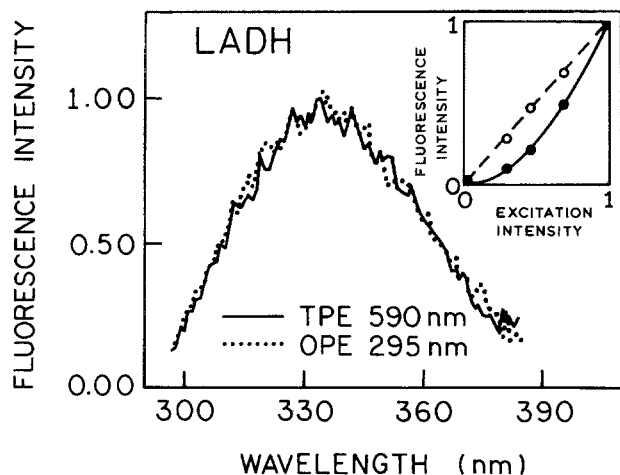


**Fig. 1.** Fluorescence emission spectra of LADH obtained for one-photon (●●●●) and two-photon (—) excitation. The inset shows the dependence of the one-photon (—○—) and two-photon-induced fluorescence intensity (—●—) on the intensity of the 295-nm (○) or 590-nm (●) incident light. The maximum intensities for OPE and TPE are both normalized to unity in the spectra and the inset.

assumed to be  $0.2^\circ$  and 0.005, respectively.<sup>(34)</sup> For analysis of the anisotropy decays the same uncertainties were assumed for the differential polarized phase and modulation ratios, respectively.<sup>(35)</sup>

## RESULTS AND DISCUSSION

### Emission Spectra of LADH for OPE and TPE

It is well-known that the emission spectra of trp-314 and trp-15 are distinct as seen from their one-photon-induced emission spectra.<sup>(1)</sup> The short-wavelength region of the LADH emission spectrum is dominated by the fluorescence of buried residue trp-314, while the fluorescence of trp-15 is red-shifted because it is located in the outer edge of the catalytic domain and exposed to solvent. Hence, we expected the emission spectra of LADH to be sensitive to the relative extent of excitation of each residue by OPE and TPE.

Emission spectra of LADH in 20 mM phosphate buffer (pH 7.5) are shown in Fig. 1 for OPE at 295 and TPE at 590 nm. For direct comparison, the OPE spectrum was recorded on the same instrument as the TPE spectrum (see Materials and Methods), except for the use of a frequency doubler for OPE. For one-photon excitation at 295 nm the emission intensity is linearly proportional (insert) to the intensity of the 295 nm incident light (—○—). Fitting of these data to a straight line  $I(\text{em})$

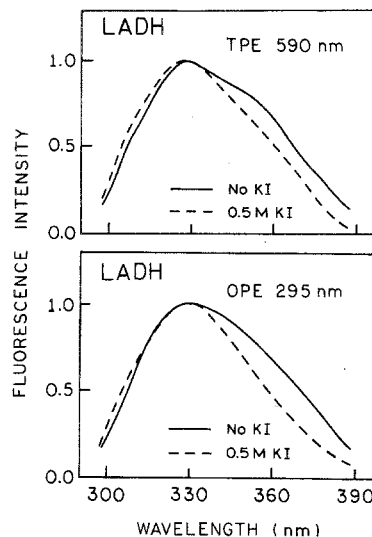


**Fig. 2.** Fluorescence emission spectra of LADH obtained for TPE (top) at 590 nm and OPE (bottom) at 295 nm in the absence (—) and in the presence of 0.5 M KI (---). The maximum intensities for all spectra are normalized to unity.

$= A_0$  (excit) yielded  $A_0 = 1.02$ . In contrast, for TPE at 590 nm, the intensity is dependent on the square of the peak laser power (—●—). Fitting of these data from Fig. 1 to  $I(\text{em}) = B_0 [I(\text{excit})]^n$  yielded  $B_0 = 0.99$  and  $n = 1.91$ . The quadratic dependence on the excitation intensity demonstrates that the observed emission is due to a biphotonic process at 590 nm. The emission spectra of LADH are similar for OPE and TPE (Fig. 1). There was also no significant difference between emission spectra for OPE at 298 and TPE at 596 nm (data not shown). The similarity of the emission spectra for OPE and TPE suggests that the two tryptophan residues are excited to a similar extent for both modes of excitation.

It is known that the exposed residue trp-15 can be preferentially quenched by water soluble quenchers.<sup>(1)</sup> Hence, in the presence of KI the emission is expected to be blue-shifted toward the shorter wavelength emission of trp-314, which is then expected to dominate the emission spectrum. We reasoned that examination of the emission spectra under these conditions could reveal selected excitation of one of the residues by two-photon excitation. Emission spectra of LADH in the presence of KI are shown in Fig. 2. The emission intensity was  $\sim 30\%$  lower with 0.5 M KI and the quenched emission spectrum is blue-shifted for OPE (Fig. 2, bottom), in agreement with published data on the OPE fluorescence of LADH.<sup>(7,8)</sup> The emission spectrum for TPE shows a similar blue shift with 0.5 M KI (Fig. 2, top). The short-wavelength part of TPE emission is again dominated by

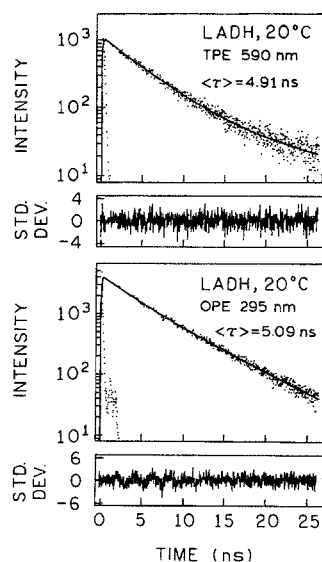


**Fig. 3.** Fluorescence intensity decays of LADH at 20°C in 20 mM phosphate buffer (pH 7.5) obtained for TPE (top) at 590 nm and OPE (bottom) at 295 nm. The dotted curves represent the profile of the excitation pulse (left) and fluorescence decay (right). The solid curves represent the theoretical values of the best three exponential fits. The goodness-of-fit parameters  $\chi_R^2$  were equal to 1.13 and 1.17, respectively.

fluorescence of tryptophan residue (trp-314). The data in Figs. 1 and 2 suggest that one- and two-photon excitation results in similar extents of excitation of the two tryptophan residues in LADH.

### Time-Resolved Intensity Decays With One- and Two-Photon Excitation

Another measure of the relative proportions of excitation of the two tryptophan residues in LADH was obtained from the time-resolved emission spectra. It is known that the residues display distinct lifetimes of 7.45 and 3.95 ns for trp-15 and -314,<sup>(13)</sup> respectively. This fact, coupled with the different emission spectra of each residue, suggests that the time-resolved intensity decays and/or emission spectra should provide a sensitive indicator of the degree of excitation of each residue. We measured the fluorescence intensity decays resulting from TPE at 590 nm of 0.26 mM LADH in 20 mM phosphate buffer (pH 7.5) at 20°. These decays were measured at different emission wavelengths with a spectral resolution of 4 nm. Typical intensity decays profiles for OPE at 295 nm and TPE at 590 nm are presented in Fig. 3. Measurements were performed for different emission wavelengths in the range of 305–385 nm for OPE and 315–380 nm for TPE. The narrow range of emission

wavelengths for TPE is due to the very low fluorescence intensity below 310 and above 380 nm, where we were not able to obtain reliable decay data. The  $\alpha_i$ ,  $\tau_i$ ,  $f_i$ , and  $\langle \tau \rangle$  value for OPE 295 nm (Table I) and for TPE 590 nm (Table II) are also shown for selected wavelengths. Examination of Tables I and II revealed that similar decay times and amplitudes were observed for OPE and TPE. While some differences in the  $\alpha_i$  and  $\tau_i$  values were found for OPE and TPE for some emission wavelengths, it is difficult to recover their values for a three exponential decay. We are not certain of the origin of the short component (0.1 to 0.2 ns) in the intensity decays of LADH (Tables I and II), which could be due to spectral relaxation during the excited state lifetime or quenching processes within the protein. Nonetheless, the amplitude of this component is low, and the intensity decay is dominated by the 2-ns decay times thought to be representative of the two tryptophan residues. The intensity decay data are more reliable compared by examination of the mean decay times (Fig. 4). As expected, the decay times increase with increasing observation wavelengths. However, the mean decay times for OPE and TPE are similar at all wavelengths (Fig. 4), suggesting a similar fractional contribution of each residue for OPE and TPE, in the range of 305–385 nm for OPE and 315–380 nm for TPE.

### Time-Resolved Emission Spectra of LADH

The data in Tables I and II were used to calculate the time-resolved emission spectra. These spectra result from numerical calculation of the time-resolved decays measured for 0.26 mM LADH in 20 mM phosphate buffer (pH 7.5) at 20°. The time-resolved emission spectra at times ranging from 0.1 to 18 ns are essentially the same for OPE and TPE (Fig. 5). The fluorescence at 310–320 nm, which is dominated by emission from trp-314, decays much faster than at 330–380 nm, which is mainly from trp-15 (Fig. 4). The similarity of the time-resolved emission spectra for OPE and TPE again suggests similar relative excitation for both modes of excitation.

### Excitation Anisotropy Spectra of LADH

The excitation anisotropy spectrum of tryptophan is known to be strongly dependent on the excitation wavelength. It was reported previously that the excitation anisotropy spectrum for TPE of indole and *N*-acetyltryptophanamide was quite distinct from that observed for OPE.<sup>(23)</sup> Hence, it was of interest to compare the excitation anisotropy spectrum of LADH. Excitation anisot-

**Table I.** Multiexponential Analysis of LADH Fluorescence Intensity Decays Resulting from OPE at 295 nm [Intensity decays were measured for 0.26 mM LADH in 20 mM Phosphate Buffer (pH 7.5) at 20°C Using Time-Correlated Single-Photon Counting]

Emission wavelength (nm)	$\alpha_i$	$f_i^a$	$\tau_i$ (ns)	$\langle\tau\rangle$ (ns) <sup>b</sup>	$\chi^2_R$		
					1 exp.	2 exp.	3 exp.
308	0.308	0.009	0.092	4.58	1.14	1.09	1.00
	0.205	0.160	2.444				
	0.513	0.830	5.045				
318	0.195	0.009	0.172	4.88	1.43	1.15	1.11
	0.370	0.304	2.987				
	0.434	0.687	5.778				
328	0.158	0.007	0.158	4.90	2.21	1.45	1.28
	0.256	0.159	2.330				
	0.586	0.837	5.415				
338	0.125	0.006	0.184	5.09	2.34	1.24	1.18
	0.281	0.175	2.553				
	0.594	0.820	5.669				
348	0.185	0.006	0.126	5.40	2.84	1.46	1.31
	0.345	0.193	2.053				
	0.470	0.800	6.245				
358	0.097	0.004	0.192	5.44	2.00	1.19	1.16
	0.233	0.123	2.393				
	0.671	0.873	5.898				
368	0.118	0.003	0.134	5.77	1.73	1.19	1.17
	0.267	0.157	2.734				
	0.615	0.840	6.363				
378	0.087	0.005	0.281	6.29	1.52	1.15	1.12
	0.398	0.282	3.761				
	0.515	0.713	7.332				
388	0.166	0.003	0.105	6.93	1.47	1.19	1.17
	0.288	0.197	3.620				
	0.546	0.800	7.766				

$$^a f_i = \alpha_i \tau_i / \sum_j \alpha_j \tau_j$$

$$^b \langle\tau\rangle = \sum_i f_i \tau_i$$

ropy spectra of 0.26 mM LADH in 20 mM phosphate buffer (pH 7.5) containing 70% glycerol at  $-60^\circ\text{C}$  are presented in Fig. 6. These spectra were measured for OPE at 285–305 nm and TPE at 570–610 nm, and for 313- and 340-nm emission wavelengths. The emission wavelengths were chosen to obtain emission dominated by trp-314 or trp-15, respectively. The OPE anisotropy spectrum for 340-nm emission has the same features as for 313 nm. This structure is typical for tryptophan-containing proteins.<sup>(36)</sup> Limiting-anisotropy values obtained for 340-nm emission are lower than for 313 nm for both modes of excitation. The anisotropy values obtained for OPE at 295 nm agree very well with the already published steady-state anisotropy values for these fluorophores,<sup>(14)</sup> which are 0.21 and 0.265 for trp-15 and trp-314, respectively.

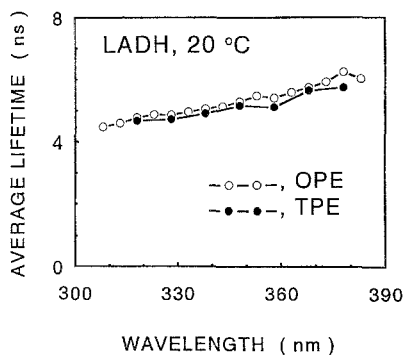
The TPE anisotropy values are several times lower than the OPE anisotropy values and the structures of TPE and OPE anisotropy spectra are different. As discussed by Callis, there is no unique relationship between the OPE and the TPE anisotropy values.<sup>(37)</sup> We are surprised that the anisotropies of LADH are lower than those observed previously for *N*-acetyl-L-tryptophanamide under similar conditions.<sup>(23)</sup> In fact,  $r_0$  values as low as 0.1 were observed for 5-methoxyindole,<sup>(15)</sup> compared to 0.28 for OPE. Hence, the low anisotropies observed for LADH are not unexpected, but further analysis is required to determine if these values reflect effects of the proteins on the indole residues. The present results suggest that low TPE anisotropy values appear to be characteristic of indoles, for both solvent-exposed and buried residues.

**Table II.** Multiexponential Analysis of LADH Fluorescence Intensity Decays Resulting from TPE at 590 nm [Intensity Decays Were Measured for 0.26 mM LADH in 20 mM phosphate buffer (pH 7.5) at 20°C Using TCSPC]

Emission wavelength (nm)	$\alpha_i$	$f_i^a$	$\tau_i$ (ns)	$\langle\tau\rangle$ (ns) <sup>b</sup>	$\chi_R^2$		
					1 exp.	2 exp.	3 exp.
318	0.270	0.013	0.159	4.67	1.14	1.06	1.04
	0.372	0.365	3.187				
	0.358	0.622	5.640				
328	0.550	0.013	0.046	4.72	1.31	1.06	1.00
	0.078	0.077	2.039				
	0.372	0.910	5.013				
338	0.553	0.015	0.055	4.91	1.50	1.19	1.12
	0.133	0.166	2.600				
	0.314	0.819	5.460				
348	0.506	0.012	0.058	5.16	1.21	1.15	1.07
	0.148	0.158	2.552				
	0.346	0.830	5.734				
358	0.707	0.015	0.030	5.12	1.34	1.04	0.99
	0.060	0.098	2.350				
	0.233	0.887	5.508				
368	0.723	0.016	0.031	5.65	1.35	1.21	1.16
	0.160	0.408	3.729				
	0.117	0.576	7.157				
378	0.799	0.018	0.024	5.75	1.29	1.17	1.11
	0.063	0.153	2.608				
	0.138	0.829	6.456				

$$^a f_i = \alpha_i \tau_i / \sum_j \alpha_j \tau_j$$

$$^b \langle\tau\rangle = \sum f_i \tau_i$$

**Fig. 4.** Wavelength dependence of the average lifetime of LADH fluorescence obtained for one-photon (○) and for two-photon (●) excitation at 295 and 590 nm, respectively.

### Anisotropy Decay of LADH

Frequency-domain anisotropy decay data for LADH at 10 and 20°C are presented in Fig. 7 and Table III. When analyzed individually, the OPE data at 300 nm and TPE data at 600 nm yielded slightly different correlation times (Table III). However, global analysis

for OPE and TPE data yielded a good fit with the same single correlation time ( $\theta = 52$  ns) and  $\chi_R^2 = 2.1$  (Fig. 7 and Table III). The values of  $\chi_R^2$  did not decrease further for a two-correlation time model. An increase in temperature from 10 to 20°C resulted in a shorter correlation time, which is the same for OPE at 295 and 300 nm. The anisotropy decay does not contain a short correlation time, which usually reflects a segmental motion of the tryptophan residue in a typical tryptophan-containing protein. Observations of a single correlation time and the absence of tryptophan segmented motion are in agreement with earlier studies of LADH dynamics.<sup>(38,39)</sup> The initial anisotropies obtained from the frequency-domain data agrees with the values measured in vitrified solutions (Fig. 5). The initial anisotropies for TPE are much lower than for OPE, as observed for the excitation anisotropy spectra (Fig. 6). The similar correlation times for OPE and TPE, and in particular the absence of a short correlation time in the two-photon-induced anisotropy decay, argues against any significant heating and/or denaturation of LADH by the locally intense illumination required for TPE.

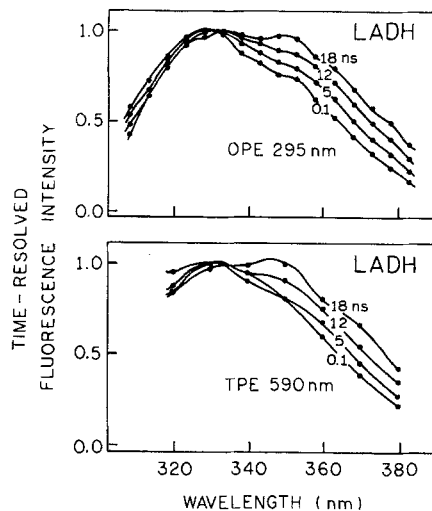


**Fig. 5.** Time-resolved emission spectra for LADH in 20 mM phosphate buffer (pH 7.5) at 20°C for 295-nm excitation (OPE; top) and 590-nm excitation (TPE; bottom). Emission spectra were calculated at the indicated times. The dots are at wavelengths where fluorescence intensity decays were measured.

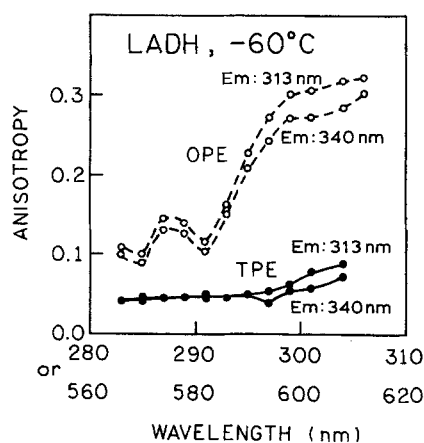


**Fig. 6.** Excitation anisotropy spectra from 0.26 mM LADH in 20 mM phosphate buffer (pH 7.5) containing 70% glycerol at  $-60^{\circ}\text{C}$  obtained for emission at 313 and 340 nm and for one-photon ( $\circ$ ) and two-photon ( $\bullet$ ) excitation, respectively.

## DISCUSSION

What are the potential advantages of two-photon excitation for studies of the structure and dynamics of proteins? One possible advantage is the larger time-zero anisotropy ( $r_0$ ) observed for fluorophores such as 2,5-diphenyloxazole,<sup>(40)</sup> 1,6-diphenylhexatriene,<sup>(20)</sup> and 4',6-diamidino-2-phenylindole.<sup>(21)</sup> Larger values of the initial anisotropy can be expected to yield improved resolution of complex anisotropy decays. Unfortunately, the initial

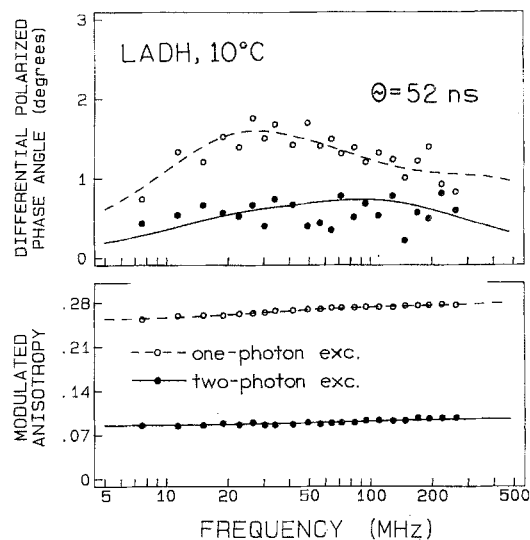


**Fig. 7.** Frequency-domain anisotropy data for the tryptophan emission from 0.5 mM LADH in 20 mM phosphate buffer (pH 7.5) at  $10^{\circ}\text{C}$  for excitation at 300 nm ( $\circ$ ) and 600 nm ( $\bullet$ ). The best global fit with one correlation time ( $\theta = 52$  ns) and  $\chi^2_R = 2.1$  is represented by the solid and dashed lines for one- and two-photon excitation, respectively. Experimental conditions are described under Fluorescence Spectroscopic Methods and in Table III.

**Table III.** Anisotropy Decay Analysis of LADH Fluorescence in 20 mM Phosphate Buffer (pH 7.5) at 10 and  $20^{\circ}\text{C}$ <sup>a</sup> (Anisotropy Decays Were Measured Using Frequency-Domain Fluorometry)

Excitation	$r_0$	$\theta$ (ns)	$\chi^2_R$
Temperature, $10^{\circ}\text{C}$			
OPE, 300 nm	0.277 (0.001)	53.3 (1.6)	1.8
TPE, 600 nm	0.094 (0.001)	40.0 (3.5)	2.2
Global OPE	0.277 (0.001)		
Global TPE	0.093 (0.001)	52.0 (1.6)	2.1
Temperature, $20^{\circ}\text{C}$			
OPE			
295 nm	0.177 (0.001)	26.5 (1.5)	1.3
300 nm	0.297 (0.001)	29.1 (1.3)	1.6

<sup>a</sup> Standard deviation values (in parentheses) represent the 67% confidence intervals. Emission was selected using two Corning 7-54 filters (each 3 mm thick) and one cutoff filter at 320 nm.

anisotropies ( $r_0$ ) for indole derivatives,<sup>(23)</sup> the single tryptophan protein human serum albumin,<sup>(15)</sup> and LADH are similar or smaller for TPE than for OPE. As a caveat, we note that it is possible that the different anisotropy spectra for one- and two-photon excitation may eventually provide advantages in the analysis of complex anisotropy decays. If the electronic transitions for one- and two-photon excitation have different orientations within the molecular frame, then global analysis of the anisot-



ropy decays from OPE and TPE may provide increased resolution of the rotational motions of asymmetric or hindered rotators. This topic is currently under investigation.

A second possible advantage of TPE could be different sensitivity to solvent for the one-photon and two-photon transition. The data for LADH suggest that such differences are minor. However, since LADH contains both a solvent-exposed and a shielded tryptophan residue, this suggests that differences in OPE and for TPE will be minor. Of course, more detailed studies may detect different excitation spectra for tryptophan residues in proteins, but to an initial approximation, these spectra appear to be similar for one- or two-photon excitation.

One possible advantage of the above results is an easier comparison of the spectral data for OPE and TPE of proteins. For instance, TPE has been used in fluorescence microscopy<sup>(41)</sup> and in pattern photobleaching with evanescent illumination.<sup>(42)</sup> The use of TPE allows the use of long-wavelength sources for excitation of protein fluorescence. In these cases one can expect similar intensity decay for OPE and TPE, which should facilitate comparisons of the data from both types of experiments.

## ACKNOWLEDGMENTS

This work was supported by Grants RR-08119 and RR-10416 from the National Institutes of Health, by Grant MCB-8804931 from the NSF, and by Grant UM-141 from the Government Committee for Scientific Research (KBN, Poland). Dr. Borys Kierdaszuk is indebted to the Fulbright Scholar Program for an Advanced Research Grant.

## REFERENCES

1. M. R. Eftink (1992) *Adv. Biophys. Chem.* **2**, 81–114.
2. H. Eklund, B. Nordstrom, E. Zeppezauer, G. Soderlund, I. Ohlsson, T. Boiwe, B.-O. Soderberg, O. Tapia, and C.-I. Branden (1976) *J. Mol. Biol.* **102**, 27–59.
3. C.-I. Branden, H. Jornvall, H. Eklund, and B. Furugren (1975) *Enzymes* **11**, 104–190.
4. H. Eklund, J.-P. Samama, L. Wallen, C.-I. Branden, A. Akesson, and T. A. Jones (1981) *J. Mol. Biol.* **146**, 561–587.
5. H. Eklund, J.-P. Samama, and T. A. Jones (1984) *Biochemistry* **23**, 5982–5996.
6. G. Petterson (1987) *Crit. Rev. Biochem.* **21**, 349–389.
7. M. A. Abdullah, J. F. Biellmann, Pl. Wiget, R. Joppich-Kuhn, and P. L. Luisi (1978) *Biochemistry* **89**, 397–405.
8. W. R. Laws and J. D. Shore (1978) *J. Biol. Chem.* **253**, 8593–8597.
9. M. R. Eftink and L. A. Selvidge (1982) *Biochemistry* **21**, 117–125.
10. J. R. Knutson, D. G. Walbridge, and L. Brand (1982) *Biochemistry* **21**, 4671–4679.
11. M. R. Eftink, Z. Wasylewski, and C. A. Ghiron (1987) *Biochemistry* **26**, 8338–8346.
12. M. R. Eftink and D. M. Jameson (1982) *Biochemistry* **21**, 4443–4449.
13. J. M. Beechem, J. R. Knutson, J. B. A. Ross, B. V. Turner, and L. Brand (1988) *Biochemistry* **22**, 6054–6058.
14. M. R. Eftink and K. A. Hagaman (1986) *Biochemistry* **25**, 6631–6637.
15. J. R. Lakowicz and I. Gryczynski (1992) *Biophys. Chem.* **45**, 1–6.
16. R. R. Birge, L. P. Murray, B. M. Pierce, H. Akita, V. Balogh-Nair, L. A. Finsen, and K. Nakanishi (1985) *Proc. Natl. Acad. Sci. USA* **82**, 4117–4121.
17. R. R. Birge (1981) *Annu. Rev. Biophys. Bioeng.* **10**, 315–354.
18. G. W. Stubbs, J. C. Saari, and S. J. Futterman (1979) *J. Biol. Chem.* **254**, 8529–8533.
19. J. Eccles and B. Honig (1983) *Proc. Natl. Acad. Sci. USA* **80**, 4959–4962.
20. J. R. Lakowicz, I. Gryczynski, J. Kusba, and E. Danielsen (1992) *J. Fluoresc.* **2**, 247–258.
21. J. R. Lakowicz and I. Gryczynski (1992) *J. Fluoresc.* **2**, 117–121.
22. B. Kierdaszuk, I. Gryczynski, A. Modrak-Wojcik, A. Bzowska, D. Shugar, and J. R. Lakowicz (1995) *Photochem. Photobiol.* **61**, 319–324.
23. J. R. Lakowicz, I. Gryczynski, E. Danielsen, and J. Frisoli (1992) *Chem. Phys. Lett.* **194**, 282–287.
24. D. J. Cannon and R. H. McKay (1969) *Biochem. Biophys. Res. Commun.* **35**, 403–707.
25. B. L. Vallee and F. L. Hoch (1955) *Proc. Natl. Acad. Sci. USA* **41**, 327–332.
26. D. V. O'Connor and D. Philips, in *Time-Correlated Single Photon Counting* (Academic Press, London, 1984).
27. D. J. S. Birch and R. E. Imhof (1991) in J. R. Lakowicz (Ed.), *Topics in Fluorescence Spectroscopy, Vol. 1. Techniques*, Plenum Press, New York, pp. 1–95.
28. J. H. Easter, R. P. De Toma, and L. Brand (1976) *Biophys. J.* **16**, 571–583.
29. J. R. Lakowicz, H. Cherek, G. Laczko, and E. Gratton (1984) *Biochim. Biophys. Acta* **777**, 183–193.
30. J. R. Lakowicz, G. Laczko, and I. Gryczynski (1986) *Rev. Sci. Instrum.* **57**, 2499–2506.
31. G. Laczko, J. R. Lakowicz, I. Gryczynski, Z. Gryczynski, and H. Malak (1990) *Rev. Sci. Instrum.* **61**, 2331–2337.
32. J. R. Lakowicz, E. Gratton, G. Laczko, H. Cherek, and M. Limkeman (1984) *Biophys. J.* **46**, 463–477.
33. E. Gratton, J. R. Lakowicz, B. Maliwal, H. Cherek, G. Laczko, and M. Limkeman (1984) *Biophys. J.* **46**, 479–486.
34. J. R. Lakowicz and I. Gryczynski (1991) in J. R. Lakowicz (Ed.), *Topics in Fluorescence Spectroscopy, Vol. 1. Techniques*, Plenum Press, New York, pp. 293–355.
35. B. P. Maliwal and J. R. Lakowicz (1986) *Biochim. Biophys. Acta* **873**, 161–172.
36. S. V. Konev, in *Fluorescence and Phosphorescence of Proteins and Nucleic Acids*, Plenum Press, New York, pp. 93–96.
37. P. R. Callis (1993) *J. Chem. Phys.* **99**, 27–37.
38. J. B. A. Ross, C. J. Schmidt, and L. Brand (1981) *Biochemistry* **20**, 4369–4377.
39. J. R. Lakowicz, B. P. Maliwal, H. Cherek, and A. Balter (1983) *Biochemistry* **22**, 1741–1752.
40. J. R. Lakowicz, Z. Gryczynski, E. Danielsen, and M. J. Wirth (1992) *J. Phys. Chem.* **96**, 3000–3006.
41. W. Denk, J. H. Strickler, and W. Webb (1990) *Science* **248**, 73–76.
42. Z. Huang and N. L. Thompson (1993) *Biophys. Chem.* **47**, 241–249.